

See discussions, stats, and author profiles for this publication at: <https://www.researchgate.net/publication/231654844>

Influence of Solid Surface and Functional Group on the Collapse of Carbon Nanotubes

ARTICLE *in* THE JOURNAL OF PHYSICAL CHEMISTRY C · JANUARY 2010

Impact Factor: 4.77 · DOI: 10.1021/jp910630w

CITATIONS

10

READS

75

6 AUTHORS, INCLUDING:



Qingzhong Xue

China University of Petroleum

138 PUBLICATIONS 1,974 CITATIONS

[SEE PROFILE](#)



Dan Xia

Aarhus University

29 PUBLICATIONS 285 CITATIONS

[SEE PROFILE](#)



Ming Ma

Delft University of Technology

11 PUBLICATIONS 110 CITATIONS

[SEE PROFILE](#)

Effect of Chemisorption on the Interfacial Bonding Characteristics of Graphene–Polymer Composites

Cheng Lv, Qingzhong Xue,* Dan Xia, Ming Ma, Jie Xie, and Huijuan Chen

College of Physics Science and Technology, China University of Petroleum, Dongying, Shandong 257061, People's Republic of China

Received: January 6, 2010; Revised Manuscript Received: February 25, 2010

The influence of the chemical functionalization of graphene on the interfacial bonding characteristics between graphene and polymers was investigated using molecular mechanics and molecular dynamics simulations. The simulations show the bonding energy and shear stress between graphene and the polymer increase with the increase of the concentration of functionalized groups. Our simulations indicated that some specific chemical modifications of graphene play important roles in determining the strength of interfacial bonding characteristics between graphene and the polymer. Therefore, the attachment of some suitable chemical groups with a reasonable concentration to the graphene surface may be an effective way to significantly improve the load transfer between the graphene and polymer when graphene is used to produce nanocomposites.

1. Introduction

Since the first fabrication of a single graphene sheet using a mechanical cleavage method in 2004,¹ graphene, a two-dimensional sheet of an sp²-hybridized carbon system, has been a highlighted material in the past few years due to its exceptional properties.^{2,3} The unique structure, ballistic transport under ambient condition, and the massless Dirac fermion-like charge carriers of graphene make it an ideal material for future electronics, such as field effect transistors and conductive interconnects.^{4,5} Besides, graphene also exhibits great promise for potential applications in many other technological fields, such as sensors,⁶ composites,⁷ membranes for gas separation,⁸ and hydrogen storage.⁹ After graphene was reported to be the strongest material in the world,¹⁰ and the cost of graphene is much lower, graphene has increasingly attracted attention as a promising candidate to take the position of carbon nanotubes (CNTs) in the reinforcement for polymers' mechanical, electrical, and thermal properties.

Some significant studies on graphene–polymer composites show a remarkable enhancement in electrical conductivity, strength, and thermal stability of polymer composites with an addition of small amounts of graphene.^{7,11–13} Stankovich et al.⁷ first made the polystyrene–graphene composites, which exhibit a percolation threshold of 0.1 vol % for electrical conductivity at room temperature, with a conductivity of 0.1 S m⁻¹ at only 1 vol %, and can be used in a variety of electrical applications. Ramanathan et al.¹¹ reported that 1 wt % of functionalized graphene sheets in poly(acrylonitrile) increases the glass-transition temperature (T_g) of the polymer by over 40 °C and an increase of nearly 30 °C is observed with only 0.05 wt % graphene in poly(methyl methacrylate) (PMMA). An addition of approximately 1 wt % of graphene into PMMA leads to an increase of the elastic modulus by 80% and an increase of the ultimate tensile strength by 20%. A comparative study by these workers shows that, among all the nanofiller materials considered, single-layer functionalized graphene gives the best results. Das et al.¹² have studied the mechanical properties of polyvinyl

alcohol (PVA) and PMMA composites reinforced by functionalized few-layer graphene by employing the nanoindentation technique. The addition of 0.6 wt % of graphene results in a significant increase in both the elastic modulus and the hardness. The crystallinity of PVA also increases with the addition of few-layer graphene. The epoxy matrix with a loading of nearly 25 vol % of graphene shows that the thermal conductivity is enhanced by more than 3000%, which surpasses the performance of conventional fillers that require a loading of nearly 70 vol % to achieve this value.¹³

Recently, it has been demonstrated that the high mechanical performance of the polymer composites not only depends on the inherent properties of the nanofiller, but also, more importantly, depends on the optimization of the dispersion, interface chemistry, and nanoscale morphology within the polymer matrix.^{11–15} A most significant challenging issue is the efficiency of load transfer from the polymer matrix to the graphenes, which is determined by the interfacial bonding between them. Experiments have shown several routes to establish a strong interface between the graphenes and the host matrix, such as establishing a strong covalent interface by chemical bonding between the graphenes and the polymers^{11,14} or creating the polymer crystalline layer surrounding nanofillers to enhance a noncovalent interface.^{12,15} One possible way is using chemically functionalized graphenes to improve the interfacial bonding between the graphenes and the supported matrix.

As we know, it is difficult to devise all kinds of experiments to study the interfacial characteristics of graphene–polymer composites. Therefore, molecular mechanics (MM) and molecular dynamics (MD) simulations maybe useful methods to investigate the interfacial reinforcement mechanisms of graphene–polymer composites. Recently, some groups have used MM and MD simulations to investigate the interfacial properties of CNT-reinforced polymer composites^{16–18} and found that the chemical attachment on interfacial properties of CNTs can influence greatly the physical properties of the CNT-reinforced polymer composites.^{19–21} In this study, the influence of the chemical functionalization of graphene on the interfacial bonding characteristics between graphene and the polymer was investigated using MM and MD simulations. The simulations show that some

* To whom correspondence should be addressed. E-mail: xueqingzhong@tsinghua.org.cn

specific chemical modifications of graphenes play an important role in determining the strength of interfacial bonding characteristics between the graphene and polymer. Therefore, the attachment of chemical groups with a reasonable concentration to the graphene surface may be an effective way to significantly improve the load transfer between the graphene and polymer when the graphene is used to produce nanocomposites.

2. Experimental Section

2.1. Computational Method. In this research, MM and MD simulations were conducted to explore the interfacial bonding characteristics between graphenes and polymers, through which we could get useful information for the development of graphene-based polymeric composites. Here, MM and MD simulations were carried out using a commercial software package called Materials Studio developed by Accelrys Inc. The condensed phase optimization molecular potentials for atomistic simulation studies (COMPASS) module in the Materials Studio software was used to conduct force-field computations. The COMPASS is a parametrized, tested, and validated first ab initio force field,^{22,23} which enables an accurate prediction of various gas-phase and condensed-phase properties of most of the common organic and inorganic materials.^{24–26}

2.2. Force Field. The application of quantum mechanical techniques can accurately simulate a system of interacting particles, but such techniques often cost too much time and are usually feasible only in systems containing up to a few hundreds of interacting particles. As we know, the main goal of simulations of the systems containing a large number of particles is generally to obtain the systems' bulk properties that are primarily controlled by the location of atomic nuclei, so the knowledge of the electronic structure, provided by the quantum mechanical techniques, is not critical. Thus, we could have a good insight into the behavior of a system if a reasonable, physically based approximation of the potential (force field) can be obtained, which can be used to generate a set of system configurations that are statistically consistent with a fully quantum mechanical description. As stated above, a crucial point in the atomistic simulations of multiparticle systems is the choice of the force fields, a brief overview of which is given in this section.

In general, the total potential energy of a molecular system includes the following terms:²⁷

$$E_{\text{total}} = E_{\text{valence}} + E_{\text{cross-term}} + E_{\text{nonbond}} \quad (1)$$

$$E_{\text{valence}} = E_{\text{bond}} + E_{\text{angle}} + E_{\text{torsion}} + E_{\text{oop}} + E_{\text{UB}} \quad (2)$$

$$\begin{aligned} E_{\text{cross-term}} = & E_{\text{bond-bond}} + E_{\text{angle-angle}} + E_{\text{bond-angle}} \\ & + E_{\text{end-bond-torsion}} + E_{\text{middle-bond-torsion}} \\ & + E_{\text{angle-torsion}} + E_{\text{angle-angle-torsion}} \end{aligned} \quad (3)$$

$$E_{\text{nonbond}} = E_{\text{vdW}} + E_{\text{Coulomb}} + E_{\text{H-bond}} \quad (4)$$

The valence energy, E_{valence} , generally includes a bond-stretching term, E_{bond} , a two-bond angle term, E_{angle} , a dihedral bond-torsion term, E_{torsion} , an inversion (or an out-of-plane interaction) term, E_{oop} , and a Urey–Bradley term (involves interactions between two atoms bonded to a common atom), E_{UB} . The cross-term interacting energy, $E_{\text{cross-term}}$, generally includes stretch–stretch interactions between two adjacent bonds, $E_{\text{bond-bond}}$, bend–bend interactions between two valence

angles associated with a common vertex atom, $E_{\text{angle-angle}}$, stretch–bend interactions between a two-bond angle and one of its bonds, $E_{\text{bond-angle}}$, stretch–torsion interactions between a dihedral angle and one of its end bonds, $E_{\text{end-bond-torsion}}$, stretch–torsion interactions between a dihedral angle and its middle bond, $E_{\text{middle-bond-torsion}}$, bend–torsion interactions between a dihedral angle and one of its valence angles, $E_{\text{angle-torsion}}$, and bend–bend–torsion interactions between a dihedral angle and its two valence angles, $E_{\text{angle-angle-torsion}}$. The nonbond interaction term, E_{nonbond} , accounts for the interactions between nonbonded atoms and includes the van der Waals energy, E_{vdW} , the Coulomb electrostatic energy, E_{Coulomb} , and the hydrogen-bond energy, $E_{\text{H-bond}}$.

The COMPASS force field uses different expressions for various components of the potential energy, as follows.^{24,25}

$$\begin{aligned} E_{\text{valence}} = & \sum_b [K_2(b - b_0)^2 + K_3(b - b_0)^3 + \\ & K_4(b - b_0)^4] \\ & + \sum_\theta [H_2(\theta - \theta_0)^2 + H_3(\theta - \theta_0)^3 + \\ & H_4(\theta - \theta_0)^4] \\ & + \sum_\phi [V_1[1 - \cos(\phi - \phi_1^0)] + V_2[1 - \cos \\ & (2\phi - \phi_2^0)] + V_3[1 - \cos(3\phi - \phi_3^0)]] \\ & + \sum_x K_x \chi^2 + E_{\text{UB}} \end{aligned} \quad (5)$$

$$\begin{aligned} E_{\text{cross-term}} = & \sum_b \sum_{b'} F_{bb}(b - b_0)(b' - b'_0) \\ & + \sum_\theta \sum_{\theta'} F_{\theta\theta'}(\theta - \theta_0)(\theta' - \theta'_0) \\ & + \sum_b \sum_\theta F_{b\theta}(b - b_0)(\theta - \theta_0) \\ & + \sum_b \sum_\phi F_{b\phi}(b - b_0) \times \\ & [V_1 \cos \phi + V_2 \cos 2\phi + V_3 \cos 3\phi] \\ & + \sum_{b'} \sum_\phi F_{b'\phi}(b' - b'_0)(b' - b'_0) \times \\ & [F_1 \cos \phi + F_2 \cos 2\phi + F_3 \cos 3\phi] \\ & + \sum_\theta \sum_\phi F_{\theta\phi}(\theta - \theta_0) \times \\ & [V_1 \cos \phi + V_2 \cos 2\phi + V_3 \cos 3\phi] \\ & + \sum_\phi \sum_\theta \sum_{\theta'} K_{\phi\theta\theta'} \cos \phi (\theta - \theta_0) \times \\ & (\theta' - \theta'_0) \end{aligned} \quad (6)$$

$$E_{\text{nonbond}} = \sum_{i>j} \left[\frac{A_{ij}}{r_{ij}^9} - \frac{B_{ij}}{r_{ij}^6} \right] + \sum_{i>j} \frac{q_i q_j}{\epsilon r_{ij}} + E_{\text{H-bond}} \quad (7)$$

where q is the atomic charge, ϵ is the dielectric constant, and r_{ij} is the $i-j$ atomic separation distance. b and b' are the lengths of two adjacent bonds, θ is the two-bond angle, ϕ is the dihedral torsion angle, and χ is the out-of-plane angle. b_0 , k_i ($i = 2-4$), θ_0 , H_i ($i = 2-4$), ϕ_i^0 ($i = 1-3$), V_i ($i = 1-3$), $F_{bb'}$, b'_0 , $F_{\theta\theta'}$, θ'_0 , $F_{b\theta}$, $F_{b\phi}$, $F_{\theta\phi}$, F_i ($i = 1-3$), $F_{\phi\theta\theta'}$, $K_{\phi\theta\theta'}$, A_{ij} , and B_{ij} are fitted from quantum mechanics calculations and are implemented into the

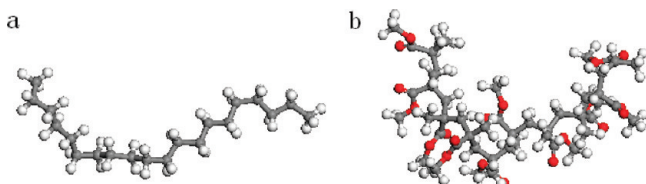


Figure 1. Molecular model of PE (a) and PMMA (b).

Discover module of Materials Studio, a powerful commercial atomic simulation program used in this paper.

2.3. Molecular Model. Due to the simplicity and genetic representation feature for polymer materials, we use polyethylene (PE) and poly(methyl methacrylate) (PMMA) as matrices, which are both well-known polymers used in a variety of engineering areas. The molecular models, PE and PMMA, with 10 repeating units in each chain, are chosen in the study (Figure 1). The single graphene sheets, which have widths of 41.82 Å and lengths of 60.36 Å, are selected for simulations of the graphene–polymer composites. The unsaturated boundary effect was avoided by adding hydrogen atoms at the ends of the graphenes.

Carboxylation is one of the common approaches to chemical functionalization of carbon materials. Through interaction with oxidizing inorganic acids, it will easily create dangling bonds on the surface of carbon materials that are progressively oxidized to hydroxyl (−OH), carbonyl (=CO), and carboxyl (−COOH) functional groups.²⁸ In the present work, we used carboxyl groups to functionalize the graphene surface and assumed the graphenes were well-dispersed in the PE and PMMA matrix. The composites, reinforced by pristine graphene and the graphenes on which 0.5, 2.5, 5, 7.5, or 10% of the carbon atoms had a bonded carboxyl group, were simulated using MM and MD simulations. The chemical functionalization of the graphene has been performed by attaching functional groups to the surface through chemical covalent bonding, and the functional groups were randomly end-grafted to the surface of the graphenes. Figure 2 shows the graphene on which 2.5% of the atoms were attached by carboxyl groups (the left panel) and the associated change in geometry of the atoms to which the carboxyl groups are bonded (the right panel). The bonded graphene atoms are “raised” away from the graphene surface. Recently, an ab initio study of carboxylated graphene with no surface defects, Stone–Wales defects, and vacancies has shown that the bonding of COOH groups to graphene clusters is significantly stronger in the presence of surface defects.²⁹ The calculated binding energy of the COOH group on graphene with no surface defects is 1.09 eV.

3. Results and Discussion

To investigate the influence of chemical functionalization on the interfacial bonding between graphene and the polymer, we used a pullout simulation.^{18,19} The bonding strength between the graphene sheet and polymer is related to the interfacial energy in the composites. Generally, the interaction energy is estimated from the difference between the potential energy of the composite system and the potential energy for the polymer molecules and the corresponding nanofillers,^{19,30,31} so it can be calculated as the difference between the minimum energy and the energy at an infinite separation of the graphene sheet and the polymer matrix as follows

$$\Delta E = E_{\text{total}} - (E_{\text{graphene}} + E_{\text{polymer}}) \quad (8)$$

where E_{total} is the total potential energy of the composite, E_{graphene} is the energy of the graphene sheet without the polymer, and E_{polymer} is the energy of the polymer without the graphene sheet. The total interaction energy, ΔE , is twice the interfacial bonding energy γ scaled by the contact area A , and for the graphene with a sheet structure, the contact area A is twice the surface area S .³²

$$\gamma = \frac{\Delta E}{2A} = \frac{\Delta E}{4S} \quad (9)$$

The magnitude of interfacial shear stress from the polymer matrix to the graphene is known to strongly influence the mechanical properties of composites. The pullout simulations were performed to characterize the interfacial shear stress of the composites. The pullout energy, E_{pullout} , is defined as the energy difference between the full embedded graphene sheet and the complete pullout configuration.³³ The pullout energy was divided into three terms as follows¹⁷

$$E_{\text{pullout}} = E_2 - E_1 = (\Delta E_2 + E_{\text{graphene}2} + E_{\text{polymer}2}) - (\Delta E_1 + E_{\text{graphene}1} + E_{\text{polymer}1}) = (\Delta E_2 - \Delta E_1) + (E_{\text{graphene}2} - E_{\text{graphene}1}) + (E_{\text{polymer}2} - E_{\text{polymer}1}) \quad (10)$$

where E_2 and E_1 are the potential energies of the composite after and before the pullout simulation, respectively, E_{graphene} and E_{polymer} are the potential energies of the graphene and the polymer, respectively, and ΔE is the interaction energy between the graphene and the polymer. The pullout energy can be related to the interfacial shear stress, τ_i , by the following relation

$$E_{\text{pullout}} = \int_{x=0}^{x=L} A\tau_i dx = \int_{x=0}^{x=L} 2S\tau_i dx = \int_{x=0}^{x=L} 2h(L-x)\tau_i dx = h\tau_i L^2 \quad (11)$$

$$\tau_i = \frac{E_{\text{pullout}}}{hL^2} \quad (12)$$

where A is the contact area, S is the surface area of the graphene, h and L are the width and length of the graphene, respectively, and x is the coordinate along the longitudinal axis.³³

In the simulations, each of the composite systems was composed of a fragment of graphene totally embedded inside the amorphous polymer matrix. A model of the composite system embedded by the pristine graphene, which consisted of a supercell in the range of 57 Å × 57 Å × 62 Å, is shown in Figure 3a. Each of the configurations was initiated by randomly generating 112 PMMA molecular chains surrounding the graphene using an initial density of 1.2 g/cm³ for the graphene–PMMA system and 369 PE molecular chains surrounding the graphene using an initial density of 0.9 g/cm³ for the graphene–PE system. The models were put into a constant-temperature, constant-pressure (NPT) ensemble simulation with a pressure of 10 atm and a temperature of 300 K for 100 ps with a time step of 1 fs while holding the graphene rigid. The purpose of this step was to slowly compress the structure of the matrix polymers to generate an initial amorphous matrix with the correct density and low residual stress. The matrix polymers were then put into a constant-temperature, constant-volume (NVT) ensemble simulation and equilibrated for 50 ps with a time step of 0.5 fs with rigid graphene. After that, the

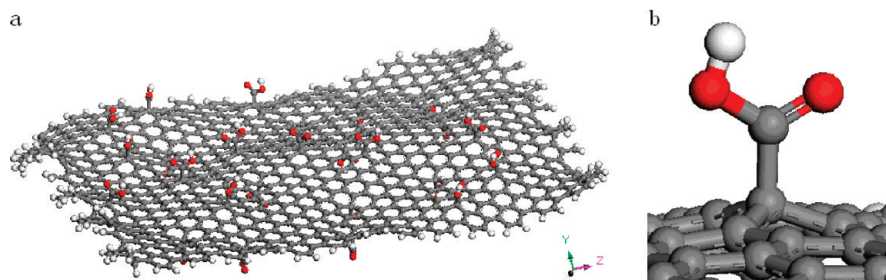


Figure 2. Illustration of graphene with carboxyl groups randomly chemisorbed to 2.5% of the carbon atoms.

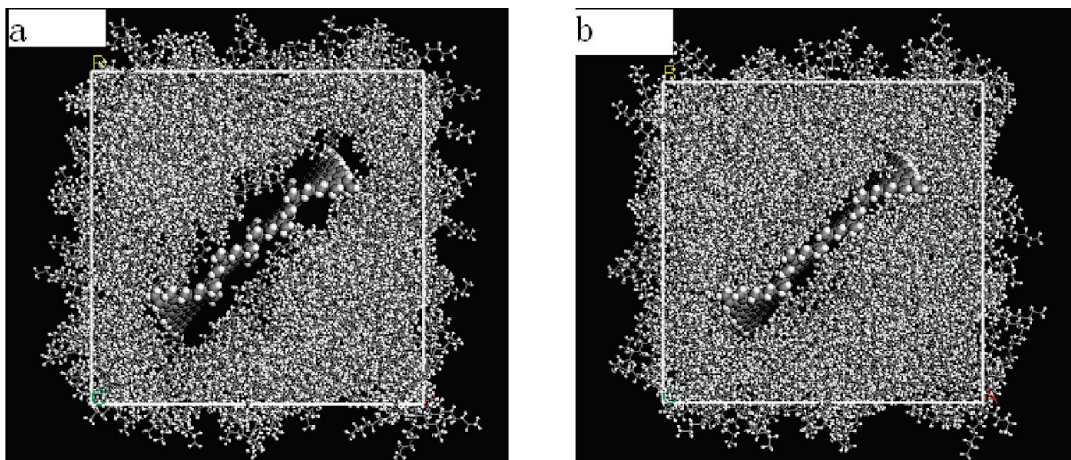


Figure 3. Cross-sectional view of the graphene–PE system before and after simulation.

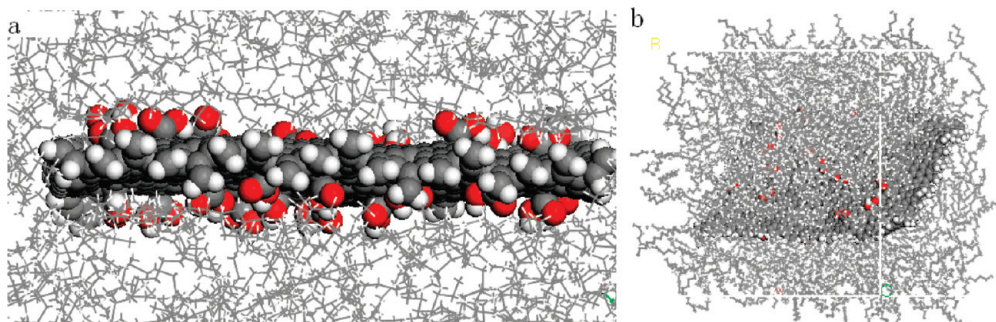


Figure 4. Illustration of the composite embedded by a graphene with carboxyl groups randomly chemisorbed to 2.5% of the carbon atoms: (a) top view and (b) side view.

composite systems were further equilibrated for 100 ps at a time step of 2 fs with nonrigid graphenes to create a zero initial stress state using NVT ensembles. The energy of the composite systems was minimized to achieve the strongest bonding between the graphene and the polymer, shown in Figures 3b and 4.^{18,30} Finally, the interfacial bonding energy and interfacial shear stress were calculated through pullout simulations.

3.1. Interfacial Bonding for Pristine Graphene. Figure 5 shows the snapshots of the pullout simulations, which were performed in order to characterize the interfacial shear strength of the composites. The graphenes were pulled out of the PE and PMMA matrix along the tangential direction of the graphene sheet. The potential energy, interaction energy, and interfacial bonding energy were plotted against the displacement of the graphenes from the PE and PMMA matrix, as shown in Figure 6. During the pullout, the interaction energy between the graphenes and the polymer changed with the displacement linearly and decreased toward a value of zero, as shown in Figure 6a. This is due to the stable interfacial binding interaction and the decrease of contact area during the pullout. Figure 6b indicates that the pullout energy of the graphene–polymer

composite system was increased as the graphenes were pulled out of the polymer. The interfacial binding energy was kept constant within 0.06–0.1 kcal/mol Å² during the pullout, as shown in Figure 6c. After the graphene was completely pulled out of the polymer, the potential energy of the system was leveled off and the interaction energy then kept at zero.

3.2. Influence of Concentration of Chemical Functionalization. The polymer composites reinforced by graphenes on which 0, 0.5, 2.5, 5, 7.5, or 10% of the carbon atoms had a bonded carboxyl group were simulated. The graphene and the polymer matrix were not held fixed in the pullout simulation. Therefore, the pullout energy has been influenced by the deformation of the graphene and polymer during the pullout. Figures 7 and 8 show that the interaction energy between the graphenes and the polymer changed with the displacement nearly linearly during the pullout, which is due to the stable interfacial binding interaction between the graphenes and the polymer. The interaction energy will keep at zero after the graphenes were completely pulled out of the polymer because there was no interaction between the graphenes and the polymer.

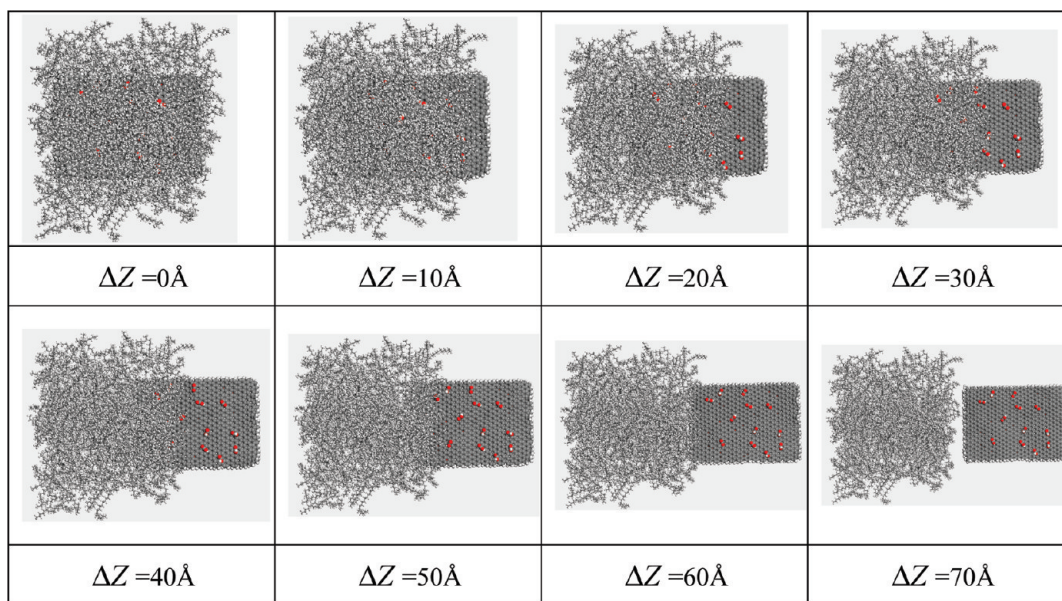


Figure 5. Snapshots from the MD simulation of the pullout of the graphene with $-COOH$ groups randomly chemisorbed to 2.5% of the carbon atoms.

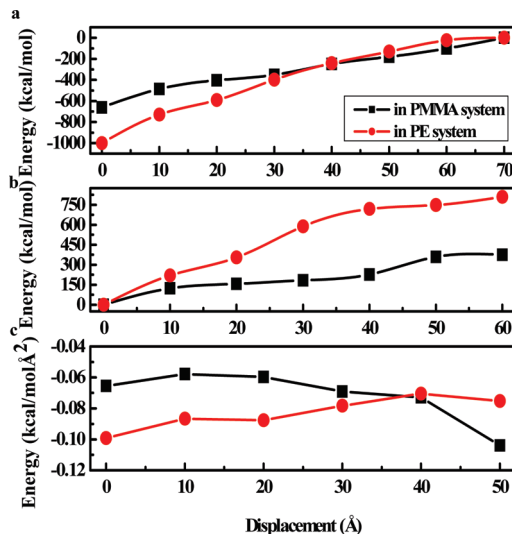


Figure 6. Energy plots during the pullout of the graphene from the PE and PMMA matrixes: (a) interaction energy, (b) pullout energy, and (c) interfacial bonding energy.

Plotted in Figure 9a,b are the calculated interaction energies and interfacial bonding energies for graphenes as a function of the degree of functionalization. When the degree of functionalization is increased, the interaction energy and interfacial bonding energy between the simulated graphene and the polymer monotonically increase toward a magnitude value, which are about 4 times the value for pristine graphene. The interfacial bonding, which appears to be critically dependent on the graphene–polymer interface surface area, will increase linearly with the total interface surface area.¹⁸ When the graphene is chemically attached with carboxyl groups, the contact area between the graphene and the polymer matrix will be drastically increased, which will cause the increase of the interfacial bonding between the graphene and the polymer.

Figure 9c shows the growth and saturation of the shear stress between the graphenes and the polymer with higher degrees of functionalization. An effective enhancement of the shear stress could be attained with the successful embedding of functionalization. When the functional groups of graphene were suc-

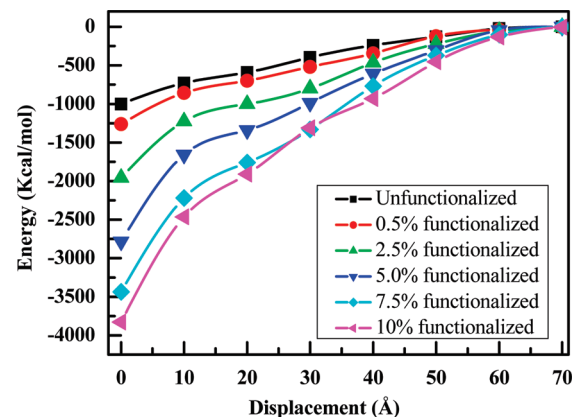


Figure 7. Interaction energy plots during the pullout of the graphene from the PE matrix.

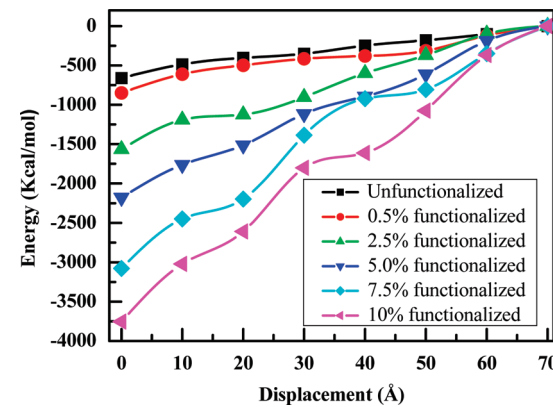


Figure 8. Interaction energy plots during the pullout of the graphene from the PMMA matrix.

cessfully embedded into the polymer matrix, which may possibly link graphene with the polymer matrix, the shear stress could be effectively increased. The shear stress of the graphene–polymer interface with weak nonbonded interactions can be increased by about 400% with the introduction of a relatively low density ($\leq 10\%$) of chemical attachment. However, when the density of functionalization becomes higher, some functional

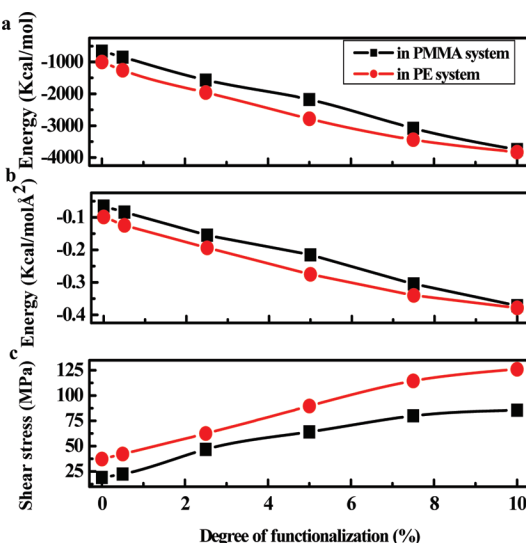


Figure 9. Influence of chemical functionalization of graphene on the interfacial bonding characteristics of the graphene–PE and graphene–PMMA systems: (a) interaction energy, (b) interfacial bonding energy, and (c) shear stress.

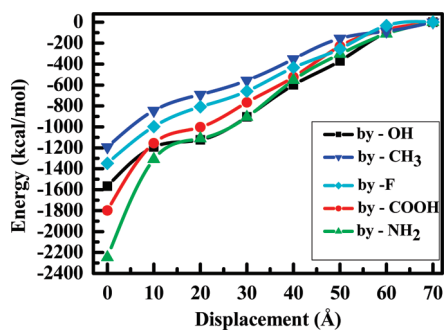


Figure 10. Interaction energy plots during the pullout of the graphene with different groups randomly chemisorbed to 2.5% of the carbon atoms from the PE matrix.

groups may only contact with the other functional groups, which may lead to a direct result that the effective contact surface area between the functional groups and the polymer matrix could not be strongly increased any more, and thus, there is only a weak increase of the shear stress. It has been reported that the shear stress increased only weakly with the introduction of a relatively high density (>5%) of chemical attachment in the CNT–polymer systems.¹⁸ The saturated degree of functionalization in the graphene–polymer systems may be more than 2 times the value for the CNT–polymer systems because of the sheet structure of graphene enlarged the contact area.

3.3. Influence of Different Chemical Functionalizations. To determine the influence of different chemical functionalizations, the polymer (PE and PMMA) composites reinforced by graphenes on which 2.5% of the carbon atoms had randomly bonded with different types of functional groups (including –COOH, –F, –OH, –NH₂, and –CH₃) were simulated. The interaction energy changed with the displacement nearly linearly during the pullout and will keep at zero after the graphenes were completely pulled out of the polymer, as shown in Figures 10 and 11. It is found that the different groups attached to graphene exhibited a similar effect on the obvious enhancement of the interfacial bonding energy between the graphenes and polymer. The effect of the groups on the interfacial bonding energies between the graphenes and polymer are as follows: –NH₂>–COOH>–OH>–F>–CH₃. The reason may be

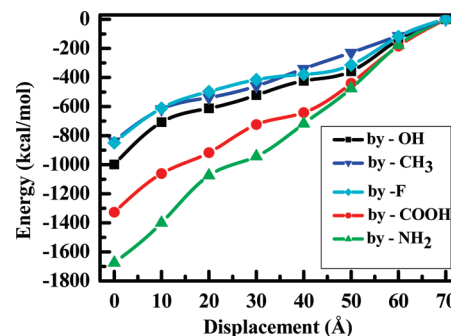


Figure 11. Interaction energy plots during the pullout of the graphene with different groups randomly chemisorbed to 2.5% of the carbon atoms from the PMMA matrix.

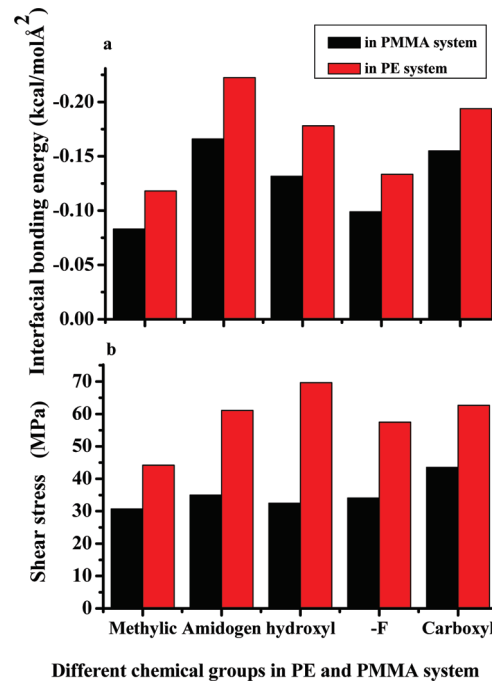


Figure 12. Influence of the graphene with different groups randomly chemisorbed to 2.5% of the carbon atoms on the interfacial bonding characteristics for the graphene–PE and graphene–PMMA systems.

the polarity of the functional groups, which need a further study using the first-principles method.

As shown in Figure 12, we find that the chemical functionalizations of graphene can significantly improve the shear stress between the graphene and polymer. One reason is that the interfacial bonding energy between the graphene and polymer, to some extent, determines the shear stress between them. In other words, the larger the interfacial bonding energy is, the larger the shear stress is. Another reason is that the shear stress is also determined by the mechanical interlocking between the graphene and the polymer matrix caused by a nanoscale surface roughness.^{11,12,34} Our simulations show that the –COOH, –OH, and –NH₂ functionalizations of graphene can improve greatly the interfacial bonding energy and shear stress between the graphene and the polymer. The interfacial bonding energy between the graphene modified by –NH₂ groups and PE (PMMA) has the strongest enhancement. However, the shear force between the graphene modified by –OH groups and PE is the strongest in the graphene–PE composites, whereas the shear force between the graphene modified by –COOH groups and PMMA is the strongest in the graphene–PMMA composites. As we know, acting as obstacles, the attached groups

themselves can play an important role in the load transfer between the graphene and polymer. For example, the shear force between the graphene modified by $-COOH$ groups and PMMA is larger than that between the graphene modified by $-NH_2$ groups and PMMA. The result may be caused by the larger obstacles of $-COOH$ groups, which can more strongly interlock with the polymer molecules to arrest the polymer chain slippage, so they exhibited a stronger shear stress. Of course, the distribution of the chemical functionalizations of the graphene also has an effect on the shear stress between the graphene and polymer.

Therefore, to enhance the shear force between graphene and the polymer, we should consider the three factors: (1) the functional groups of the graphene should largely increase the interfacial bonding energy between the graphene and the polymer, (2) the functional groups of the graphene should largely increase the mechanical interlocking between the graphene and the polymer matrix caused by a nanoscale surface roughness, and (3) the reasonable distribution of the chemical functionalizations of the graphene also has an effect on the shear stress between the graphene and polymer.

4. Conclusions

In this study, MM and MD simulations were carried out to investigate the effect of chemical functionalization on the interfacial bonding characteristics between graphene and the polymer matrix. Our simulations show that the chemical modifications of graphenes play important roles in the interfacial bonding characteristics between the graphenes and the polymer matrix, which is in accord with the experimental studies on the interfacial bonding properties of EG (expanded graphite)-PMMA and FGS (functionalized graphene sheets)-PMMA composites.¹¹ The bonding energy and shear stress between the graphene and polymer increase with the increase of the concentration of functionalized groups. Therefore, the attachment of some suitable chemical groups with a reasonable concentration to the graphene surface may be an effective way to significantly improve the load transfer between the graphenes and polymers when the graphene is used to produce nanocomposites. Furthermore, this suggests the possibility to use functionalized graphenes to effectively reinforce other kinds of polymer-based materials as well.

Acknowledgment. This work is supported by the Cultivation Fund of the Key Scientific and Technical Innovation Project, the Ministry of Education of China (708061), the Natural Science Foundation of China (10974258), and the Program for New Century Excellent Talents in University (NCET-08-0844).

References and Notes

- (1) Novoselov, K. S.; Geim, A. K.; Morozov, S. V.; Jing, D.; Zhang, Y.; Dubonos, S. V.; Grigorieva, I. V.; Firsov, A. A. *Science* **2004**, *306* (5696), 666–669.
- (2) Rao, C. N. R.; Sood, A. K.; Subrahmanyam, K. S.; Govindaraj, A. *Angew. Chem., Int. Ed.* **2009**, *48* (42), 7752–7778.
- (3) Rao, C. N. R.; Biswas, K.; Subrahmanyam, K. S.; Govindaraj, A. *J. Mater. Chem.* **2009**, *19* (17), 2457–2469.
- (4) Geim, A. K. *Science* **2009**, *324* (5934), 1530–1534.
- (5) Eda, G.; Chhowalla, M. *Nano Lett.* **2009**, *9* (2), 814–818.
- (6) Schedin, F.; Geim, A. K.; Morozov, S. V.; Hill, E. W.; Blake, P.; Katsnelson, M. I.; Novoselov, K. S. *Nat. Mater.* **2007**, *6* (9), 652–655.
- (7) Stankovich, S.; Dikin, D. A.; Dommett, G. H. B.; Kohlhaas, K. M.; Zimney, E. J.; Stach, E. A.; Piner, R. D.; Nguyen, S. T.; Ruoff, R. S. *Nature* **2006**, *442* (7100), 282–286.
- (8) Jiang, D.; Cooper, V. R.; Dai, S. *Nano Lett.* **2009**, *9* (12), 4019–4024.
- (9) Patchkovskii, S.; Tse, J. S.; Yurchenko, S. N.; Zhechkov, L.; Heine, T.; Seifert, G. *Proc. Natl. Acad. Sci. U.S.A.* **2005**, *102* (30), 10439–10444.
- (10) Lee, C.; Wei, X.; Kysar, J. W.; Hone, J. *Science* **2008**, *321* (5887), 385–388.
- (11) Ramanathan, T.; Abdala, A. A.; Stankovich, S.; Dikin, D. A.; Herrera-Alonso, M.; Piner, R. D.; Adamson, D. H.; Schniepp, H. C.; Chen, X.; Ruoff, R. S.; Nguyen, S. T.; Akasy, I. A.; Prud'Homme, R. K.; Brinson, L. C. *Nat. Nanotechnol.* **2008**, *3* (6), 327–331.
- (12) Das, B.; Prasad, K. E.; Ramamurty, U.; Rao, C. N. R. *Nanotechnology* **2009**, *20* (12), 125705.
- (13) Yu, A.; Ramesh, P.; Itkis, M. E.; Bekyarova, E.; Haddon, R. C. *J. Phys. Chem. C* **2007**, *111* (21), 7565–7569.
- (14) Fang, M.; Wang, K. G.; Lu, H. B.; Yang, Y. L.; Nutt, S. *J. Mater. Chem.* **2009**, *19* (38), 7098–7105.
- (15) Cai, D. Y.; Song, M. *Nanotechnology* **2009**, *20* (31), 315708.
- (16) Yang, M. J.; Koutsos, V.; Zaiser, M. *J. Phys. Chem. B* **2005**, *109* (20), 10009–10014.
- (17) Wei, C. Y. *Appl. Phys. Lett.* **2006**, *88* (9), 093108.
- (18) Guo, J. H.; Liang, Z. Y.; Zhang, C.; Wang, B. *Composites, Part B* **2005**, *36* (6–7), 524–533.
- (19) Zheng, Q. B.; Xue, Q. Z.; Yan, K. Y.; Gao, X. L.; Li, Q.; Hao, L. Z. *Polymer* **2008**, *49* (3), 800–808.
- (20) Chen, H. J.; Xue, Q. Z.; Zheng, Q. B.; Xie, J.; Yan, K. Y. *J. Phys. Chem. C* **2008**, *112* (42), 16514–16520.
- (21) Xie, J.; Xue, Q. Z.; Yan, K. Y.; Chen, H. J.; Xia, D.; Dong, M. D. *J. Phys. Chem. C* **2009**, *113* (33), 14747–14752.
- (22) Maple, J. R.; Hwang, M. J.; Stockfisch, T. P.; Dinur, U.; Waldman, M.; Ewig, C. S.; Hagler, A. T. *J. Comput. Chem.* **1994**, *15* (2), 162–182.
- (23) Sun, H. *J. Comput. Chem.* **1994**, *15* (7), 752–768.
- (24) Sun, H. *J. Phys. Chem. B* **1998**, *102* (38), 7338–7364.
- (25) Sun, H.; Ren, P.; Fried, J. R. *Comput. Theor. Polym. Sci.* **1998**, *8* (1/2), 229–246.
- (26) Rigby, D.; Sun, H.; Eichinger, B. E. *Polym. Int.* **1998**, *44* (3), 311–330.
- (27) Grujicic, M.; Cao, G.; Roy, W. N. *Appl. Surf. Sci.* **2004**, *227* (1–4), 349–363.
- (28) Curran, S. A.; Ellis, A. V.; Vijayaraghavan, A.; Ajayan, P. M. *J. Chem. Phys.* **2004**, *120* (10), 4886–4889.
- (29) Al-Aqtash, N.; Vasiliev, I. *J. Phys. Chem. C* **2009**, *113* (30), 12970–12975.
- (30) Gou, J. H.; Minaie, B.; Wang, B.; Liang, Z. Y.; Zhang, C. *Comput. Mater. Sci.* **2004**, *31* (3–4), 225–236.
- (31) Al-Haik, M.; Hussaini, M. Y.; Garmestani, H. *J. Appl. Phys.* **2005**, *97* (7), 074306.
- (32) Lordi, V.; Yao, N. *J. Mater. Res.* **2000**, *15* (12), 2770–2779.
- (33) Liao, K.; Li, S. *Appl. Phys. Lett.* **2001**, *79* (25), 4225–4227.
- (34) Desai, T.; Keblinski, P.; Kumar, S. K. *J. Chem. Phys.* **2005**, *122* (13), 134910.

JP100110N